Comparison of Characteristic Schemes for Three-Dimensional, Steady, Isentropic Flow

MICHAEL C. CLINE*
NASA Langley Research Center, Hampton, Va.
AND
JOE D. HOFFMAN†
Purdue University, Lafayette, Ind.

The accuracy and order of three bicharacteristic schemes based on the numerical method of characteristics for three-dimensional, steady, isentropic, supersonic flow were compared based on numerical calculations. Comparisons were made for source flows and for flows in contoured axisymmetric nozzles. The first two methods were tetrahedral line networks, differing only in the manner in which the cross derivatives were evaluated. The third method was the pentahedral line network proposed by Butler. Although all three methods were numerically stable and produced efficient and accurate solutions, Butler's method was found, in general, to be the best over-all scheme.

Introduction

CHARACTERISTICS schemes for three-dimensional, steady, isentropic flow can generally be classified as reference plane methods or bicharacteristic methods. In reference plane methods the original system of partial differential equations in three independent variables is reduced to a system of partial differential equations in two independent variables by means of approximations of the derivatives with respect to the third independent variable. These approximations to the derivatives are then treated as source or forcing terms and the resulting system of equations is solved in planes using a two-dimensional, characteristic scheme. Reference plane methods have been proposed by Ferrari,[1] Sauer,[2,3] Ferri,[4] Moretti et al.,[5,6] Katskova and Chushkin,[7] Holt,[8,9] and Rakich.[10] Reference plane methods have also been called the method of bycharacteristics,[5,6] method of near characteristics,[2] method of secondary characteristics,[3] and the method of semicharacteristics.[11] In the bicharacteristic methods the actual compatibility equations for three-dimensional flow are solved along bicharacteristics, that is, generators of the Mach conoid and streamlines. Bicharacteristic methods have been proposed by Thornhill,[12] Fowell,[13] Sauerwein,[14,15] Coburn and Dolph,[16] Holt,[17] Butler,[18] Strom,[19] and Chu.[20]

Although reference plane methods are the simpler of the two methods, the domain of dependence of the differential equations is not rigorously considered and, therefore, these methods have questionable accuracy for highly three-dimensional flows. Although bicharacteristic methods rigorously consider the domain of dependence, they require calculation of the cross derivatives in the compatibility equations, that is, differentiation in a characteristic surface and normal to the bicharacteristic direction and, therefore, are more complicated. Even though it is felt that both methods have merit, the bicharacteristic method is the more general and potentially the more accurate of the two.

The object of this study was to determine the best method in the class of bicharacteristic methods. The three bicharacteristic methods considered in this study are presented below and will hereafter be called Methods 1, 2, and 3.

Method 2 is based on the tetrahedral characteristic line network proposed by Fowell[13] and later modified by Sauerwein.[14] A variation of Method 2 was later used by Strom[19] and Sauerwein.[15] Method 1 is similar to Method 2, except the cross derivatives are calculated at both the known base points and unknown solution point by local second-order bivariate interpolation. Method 3 is the pentahedral network method proposed by Butler.[18] In all three methods, the solution is generated on successive parallel planes by first extending the streamline forward to the new solution plane determined by the Courant-Friedrichs-Lewy (C-F-L) stability criterion and then extending the bicharacteristics back to the initial-value plane. The properties at the base points are obtained by local second-order bivariate interpolating polynomials. These second-order polynomials are fit by the method of least squares to the nine initial data points shown in Figs. 1 and 2. Numerical smoothing is unavoidably introduced by the interpolation, resulting in some loss of accuracy. However, interpolation cannot be avoided in inverse schemes such as these. A complete description of these methods including the finite-difference equations for three-dimensional, steady, isentropic, nozzle flows are given below.

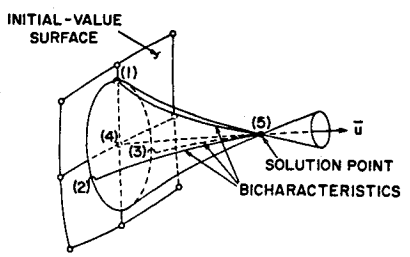

Fig. 1 Methods 1 and 2 interior point computational scheme.

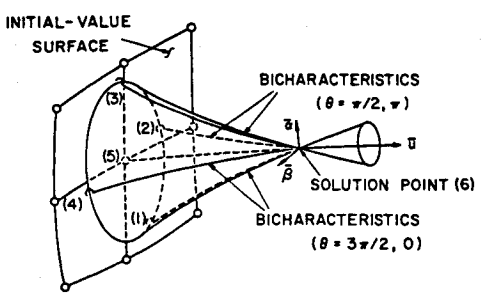

Fig. 2 Method 3 interior point computational scheme.

Presented as Paper 72-190 at the AIAA 10th Aerospace Sciences Meeting, San Diego, Calif., January 17–19, 1972; submitted February 17, 1972; revision received July 5, 1972. This work was sponsored by the Air Force Aero Propulsion Laboratory, Wright-Patterson Air Force Base, under Contract F33615-67-C-1068. The program monitor was G. J. Jungwirth (RJT).

Index categories: Supersonic and Hypersonic Flow; Nozzle and Channel Flow.

* NAS Resident Research Associate in the High-Speed Aircraft Division; formerly a Research Assistant, School of Mechanical Engineering at Purdue University. Member AIAA.

† Associate Professor of Mechanical Engineering. Member AIAA.

These three methods were first used to compute the numerical solution of spherical source flow in a conical nozzle, which was then checked against the exact solution. Second, these three methods were compared with an existing axisymmetric characteristic scheme for computing axisymmetric, steady, isentropic flow in a parabolic nozzle. From these accuracy studies some general conclusions have been drawn and are discussed.

Equations of Motion

The equations of motion for steady, inviscid, isentropic, rotational flow are

$$\rho u u_x + \rho v u_y + \rho w u_z + p_x = 0 \quad (1)$$

$$\rho u v_x + \rho v v_y + \rho w v_z + p_y = 0 \quad (2)$$

$$\rho u w_x + \rho v w_y + \rho w w_z + p_z = 0 \quad (3)$$

$$u p_x + v p_y + w p_z + \rho a^2 (u_x + v_y + w_z) = 0 \quad (4)$$

$$u P_x + v P_y + w P_z = 0 \quad (5)$$

$$u H_x + v H_y + w H_z = 0 \quad (6)$$

$$a = a(p, P, H) \quad (7)$$

Here u, v, and w are the velocity components along the x, y, and z coordinate directions, respectively, p is the pressure, ρ is the density, a is the speed of sound, P is the stagnation pressure, and H is the stagnation enthalpy. The subscripts x, y, and z, denote partial differentiation with respect to the x, y, and z coordinate directions, respectively.

Characteristic Relations

Equations (1–6) form a system of hyperbolic, partial differential equations when the flow is everywhere supersonic. The characteristic surfaces and compatibility equations, given below, are derived in detail in Ref. 21.

The characteristic surfaces are the flow stream surfaces given by

$$u n_x + v n_y + w n_z = 0 \quad (8)$$

and the wave or Mach surfaces given by

$$u n_x + v n_y + w n_z = a \quad (9)$$

where n_x, n_y, and n_z are components of the unit normals to the characteristic surfaces. The envelope of the characteristic surfaces through a point are the flow streamlines given by

$$dx/dt = u, \qquad dy/dt = v, \qquad dz/dt = w \quad (10)$$

and the wave or Mach conoid given by

$$[u^2 - (q^2 - a^2)](dx/ds)^2 + [v^2 - (q^2 - a^2)](dy/ds)^2 + [w^2 - (q^2 - a^2)](dz/ds)^2 + 2uv(dx/ds)(dy/ds) + 2uw(dx/ds)(dz/ds) + 2vw(dy/ds)(dz/ds) = 0 \quad (11)$$

where q is the velocity magnitude, t is a parameter proportional to length along a streamline, and s is a parameter proportional to length along a generator or ray of the Mach conoid. These rays of the Mach conoid are called bicharacteristics.

The compatibility equations which apply along the flow streamlines, given by Eq. (10), are

$$\rho u(u u_x + v u_y + w u_z) + \rho v(u v_x + v v_y + w v_z) + \rho w(u w_x + v w_y + w w_z) + (u p_x + v p_y + w p_z) = 0 \quad (12)$$

$$u P_x + v P_y + w P_z = 0 \quad (13)$$

$$u H_x + v H_y + w H_z = 0 \quad (14)$$

The compatibility equation which applies on the Mach surfaces and, therefore, the Mach conoid given by Eq. (11), is

$$\rho a n_x(u u_x + v u_y + w u_z) + \rho a n_y(u v_x + v v_y + w v_z) + \rho a n_z(u w_x + v w_y + w w_z) + (a n_x - u)p_x + (a n_y - v)p_y + (a n_z - w)p_z - \rho a^2(u_x + v_y + w_z) = 0 \quad (15)$$

Equation (15), when written in terms of differentiation in the bicharacteristic direction, yields

$$\rho a n_x u_t + \rho a n_y v_t + \rho a n_z w_t - p_t + \rho a^2[(n_x^2 - 1)u_x + (n_y^2 - 1)v_y + (n_z^2 - 1)w_z + (u_y + v_x)n_x n_y + (u_z + w_x)n_x n_z + (v_z + w_y)n_y n_z] = 0 \quad (16)$$

where here the subscript t denotes differentiation in the bicharacteristic direction. The term in brackets in Eq. (16) represents differentiation in a characteristic surface, but normal to the bicharacteristic direction and will hereafter be called the cross derivative. For a discussion of the other possible independent sets of compatibility equations, the reader is referred to the work of Rusanov.[22]

Method 1

Method 1 is basically a predictor-corrector scheme. A first-order predictor is used to compute a tentative solution and a second-order corrector is then used to compute the final solution. This computational scheme has been called the inverse tetrahedral scheme and is shown in Fig. 1. The solution is computed on successive constant x planes. The x locations are determined using the C-F-L stability criterion. In Fig. 1 point (4) is the intersection of the streamline with the initial-value plane, point (5) is the intersection of the streamline with the solution plane, and points (1) through (3) are the intersections of three bicharacteristics through point (5) with the initial-value plane.

Predictor

The streamline is extended from point (4) to the predetermined solution plane using the following finite-difference form of Eq. (10)

$$[x(5) - x(4)]/[t(5) - t(4)] = u(4)$$
$$[y(5) - y(4)]/[t(5) - t(4)] = v(4)$$
$$[z(5) - z(4)]/[t(5) - t(4)] = w(4) \quad (17)$$

where the numbers in parentheses denote the values at points (1) through (5) in Fig. 1. The three bicharacteristics are then extended back to intersect the initial-value plane. The points of intersection are computed by solving for $y(k)$ and $z(k)$, $k = 1, 2, 3$ from the following finite-difference form of Eq. (11)

$$\{u^2(4) - [q^2(4) - a^2(4)]\}[x(5) - x(k)]^2 + \{v^2(4) - [q^2(4) - a^2(4)]\}[y(5) - y(k)]^2 + \{w^2(4) - [q^2(4) - a^2(4)]\}[z(5) - z(k)]^2 + 2u(4)v(4)[x(5) - x(k)][y(5) - y(k)] + 2u(4)w(4)[x(5) - x(k)][z(5) - z(k)] + 2v(4)w(4)[y(5) - y(k)][z(5) - z(k)] = 0 \qquad (k = 1, 2, 3) \quad (18)$$

and the equation

$$z(4) - z(k) = Q(k)[y(4) - y(k)] \qquad (k = 1, 2, 3) \quad (19)$$

where $Q(k)$ is the desired slope of the line between points (4) and (k). The slopes, $Q(k)$, were such that the points (1), (2), and (3) were separated by angles of 120° in the initial-value plane.

The values of the dependent variable (i.e., u, v, w, p, H, and P) at points (1) through (3) are determined by interpolation. For this purpose, second-order bivariate polynomials were fit locally to nine neighboring points by the method of least squares. These nine points consist of point (4) and the eight nearest surrounding points in the initial-value plane (see Fig. 1). For reasons of numerical stability, interpolated property values were used also at point (4). The $y(k)$ and $z(k)$, $k = 1, 2, 3$ were then corrected once by replacing Eq. (18) by

$$\{u^2(k) - [q^2(k) - a^2(k)]\}[x(5) - x(k)]^2 + \{v^2(k) - [q^2(k) - a^2(k)]\}[y(5) - y(k)]^2 + \{w^2(k) - [q^2(k) - a^2(k)]\}[z(5) - z(k)]^2 + 2u(k)v(k)[x(5) - x(k)][y(5) - y(k)] + 2u(k)w(k)[x(5) - x(k)][z(5) - z(k)] + 2v(k)w(k)[y(5) - y(k)][z(5) - z(k)] = 0 \qquad (k = 1, 2, 3) \quad (20)$$

where now the values of the dependent variables in the coefficients are the previously interpolated values.

The values of $u(5)$, $v(5)$, $w(5)$, $p(5)$, $P(5)$, and $H(5)$ were then computed by solving the following finite-difference forms of Eqs. (12, 13, 14, and 16), respectively

$$\rho(4)u(4)[u(5) - u(4)] + \rho(4)v(4)[v(5) - v(4)] + \rho(4)w(4)[w(5) - w(4)] + p(5) - p(4) = 0 \quad (21)$$

$$P(4) = P(5) \quad (22)$$

$$H(4) = H(5) \quad (23)$$

$$\rho(k)a(k)n_x(k)[u(5) - u(k)]/[t(5) - t(k)] + \rho(k)a(k)n_y(k)[v(5) - v(k)]/[t(5) - t(k)] + \rho(k)a(k)n_z(k)[w(5) - w(k)]/[t(5) - t(k)] - [p(5) - p(k)]/[t(5) - t(k)] + \rho(k)a^2(k)\{[n_x^2(k) - 1]u_x(k) + [n_y^2(k) - 1]v_y(k) + [n_z^2(k) - 1]w_z(k) + [u_y(k) + v_x(k)]n_x(k)n_y(k) + [u_z(k) + w_x(k)]n_x(k)n_z(k) + [v_z(k) + w_y(k)]n_y(k)n_z(k)\} = 0 \quad (k = 1, 2, 3) \quad (24)$$

The values of the derivatives in the braces are computed by first differentiating the second-order interpolating polynomials to determine the derivatives with respect to y and z and then using the original equations of motion to determine the derivatives with respect to x.

The boundary point scheme is the same except that Eqs. (18) and (19) for $k = 1$ are replaced by the condition that point (5) must lie on a prescribed surface and Eq. (24) for $k = 1$ is replaced by

$$\bar{n}_x u(5) + \bar{n}_y v(5) + \bar{n}_z w(5) = 0 \quad (25)$$

where $(\bar{n}_x, \bar{n}_y, \bar{n}_z)$ is the unit outer normal to the boundary at point (5). The $Q(k)$, $k = 2, 3$, will now vary along the boundary. The predictor is successively repeated until the entire solution plane has been computed.

Corrector

The corrector uses the same finite-difference equations as the predictor except that all dependent variables in the coefficients of Eqs. (17–24) are replaced by values which are the average of the values at points (1), (2), (3), or (4), and the value computed at point (5) by the predictor. The cross derivatives in Eq. (24) require special attention. To determine the cross derivatives at point (5), second-order bivariate interpolating polynomials are fit locally to the predicted solution plane. The polynomials are differentiated to obtain the derivatives with respect to y and z and then the original equations of motion are used to determine the derivatives with respect to x. The derivatives in the cross derivative term in Eq. (24) are then replaced by the average of the derivatives at points (1), (2), (3), or (4), and the newly computed derivatives at point (5). The corrector then follows the same procedure as the predictor and is either applied once or iterated until a convergence criterion is satisfied for each new solution point.

Method 2

The predictor of Method 2 is the same as that of Method 1. The corrector is the same, except for the evaluation of the cross derivatives in Eq. (24). Instead of calculating the cross derivatives at each base and solution point and then averaging them, an average cross derivative for the entire interval is determined by calculating the derivatives u_x, u_y, u_z, v_x, v_y, v_z, w_x, w_y, and w_z, which make up the cross derivatives, from the equations

$$u(5) - u(k) = u_x[x(5) - x(k)] + u_y[y(5) - y(k)] + u_z[z(5) - z(k)] \quad (k = 1, 2, 3) \quad (26)$$

$$v(5) - v(k) = v_x[x(5) - x(k)] + v_y[y(5) - y(k)] + v_z[z(5) - z(k)] \quad (k = 1, 2, 3) \quad (27)$$

$$w(5) - w(k) = w_x[x(5) - x(k)] + w_y[y(5) - y(k)] + w_z[z(5) - z(k)] \quad (k = 1, 2, 3) \quad (28)$$

Therefore, the second-order interpolating polynomials are used to calculate the properties and the cross derivatives for the predictor, and the properties only for the corrector. The corrector may be applied once or iterated until a convergence criterion is satisfied for each new solution point.

The boundary point scheme is the same as that of Method 1 where $k = 4$ is used in place of the missing $k = 1$ in Eqs. (26–28).

Method 3

Butler's method[18] will be briefly outlined herein using rectangular Cartesian index notation where $x_1 = x$, $x_2 = y$, $x_3 = z$, $u_1 = u$, $u_2 = v$, $u_3 = w$, and repeated indices imply summation. For a complete development of Butler's method, the reader is referred to Refs. 18 and 23. The tangency condition used by both Butler[18] and Ransom et al.[23] to insure second-order accuracy was later found to be unnecessary by Butler[24] and, therefore, is not presented herein.

Butler's method differs from Methods 1 and 2 in the treatment of the cross derivatives. In this method the cross derivatives are eliminated at the solution point. By using a fourth bicharacteristic along with an additional "noncharacteristic relation," Butler was able to obtain three difference equations, none of which contain the solution point cross derivatives, which can be used in place of the three wave surface compatibility difference equations of Methods 1 and 2. This method is not to be confused with the redundant schemes of Sauerwein[15] and Strom.[19] These redundant methods are essentially Method 2 used repeatedly at a point. In these methods two sets of three bicharacteristics are used to compute two solutions. These solutions are then averaged to determine the final solution.

Butler introduced the following bicharacteristic parameterization (see Fig. 2)

$$dx_i = (u_i + c\alpha_i \cos\theta + c\beta_i \sin\theta)\,dt \quad (i = 1, 2, 3) \quad (29)$$

where t is a parameter proportional to length along the bicharacteristic curve, u_i/q, α_i, and β_i form an orthonormal vector set where q is the velocity magnitude, c is given by

$$c = [q^2a^2/(q^2 - a^2)]^{1/2} \quad (30)$$

where a denotes the speed of sound, and θ is a parameter corresponding to a particular bicharacteristic. Using this parameterization, Eq. (16) can be written as

$$d_l p + \rho c(\alpha_i \cos\theta + \beta_i \sin\theta)\,d_l u_i = -\rho c^2(\alpha_i \sin\theta - \beta_i \cos\theta)(\alpha_j \sin\theta - \beta_j \cos\theta)(\partial u_i/\partial x_j) \quad (31)$$

where the operator $d_l p$ denotes the derivative of p in a direction l tangent to the bicharacteristics. Butler also developed a noncharacteristic relation given by

$$d_u p = -\rho c^2(\alpha_i\alpha_j + \beta_i\beta_j)(\partial u_i/\partial x_j) \quad (32)$$

where $d_u p$ denotes the derivative of p in a direction tangent to the flow streamlines.

Equation (31) is then written along the four bicharacteristics specified by $\theta = 0$, $\pi/2$, π, and $3\pi/2$. Denote these results as Eqs. (31-1), (31-2), (31-3), and (31-4). These four equations, along with Eq. (32), form a system of five equations. Rusanov[22] showed that a maximum of three compatibility equations [i.e., Eq. (31) applied along three bicharacteristics given by Eq. (29)] are independent at a point. Thus, only three of the aforementioned system of five equations are independent. The three independent equations, which are the basis for the present scheme, are obtained as follows. Equations (31-1) through (31-4) and (32) are first written in finite-difference form by replacing the differentials by differences and the coefficients by averages of the coefficients at point (6) and the five base points (see Fig. 2). Then Eq. (31-3) is subtracted from (31-1), Eq. (31-4) is subtracted from (31-2), and Eq. (32) is subtracted from the sum of (31-1) and (31-2). This yields three independent equations in which the cross-derivatives at point (6) have been eliminated. These equations are

$$2[p(6) - p(1)]/[t(6) - t(1)] + [\rho(6)c(6)\alpha_i(6) + \rho(1)c(1)\alpha_i(6)][u_i(6) - u_i(1)]/[t(6) - t(1)] + 2[p(6) - p(3)]/[t(6) - t(3)] + [\rho(6)c(6)\alpha_i(6) + \rho(3)c(3)\alpha_i(6)][u_i(6) - u_i(3)]/[t(6) - t(3)] = -\rho(1)c^2(1)\beta_i(6)\beta_j(6)\,\partial u_i/\partial x_j(1) + \rho(3)c^2(3)\beta_i(6)\beta_j(6)\,\partial u_i/\partial x_j(3) \quad (33)$$

$$2[p(6) - p(2)]/[t(6) - t(2)] + [\rho(6)c(6)\beta_i(6) + \rho(2)c(2)\beta_i(6)][u_i(6) - u_i(2)]/[t(6) - t(2)] - 2[p(6) - p(4)]/[t(6) - t(4)] + [\rho(6)c(6)\beta_i(6) + \rho(4)c(4)\beta_i(6)][u_i(6) - u_i(4)]/[t(6) - t(4)] = -\rho(2)c^2(2)\alpha_i(6)\alpha_j(6)\,\partial u_i/\partial x_j(2) + \rho(4)c^2(4)\alpha_i(6)\alpha_j(6)\,\partial u_i/\partial x_j(4) \quad (34)$$

$$2[p(6) - p(1)]/[t(6) - t(1)] + [\rho(6)c(6)\alpha_i(6) + \rho(1)c(1)\alpha_i(6)][u_i(6) - u_i(1)]/[t(6) - t(1)] + 2[p(6) - p(2)]/[t(6) - t(2)] + [\rho(6)c(6)\beta_i(6) + \rho(2)c(2)\beta_i(6)][u_i(6) - u_i(2)]/[t(6) - t(2)] - 2[p(6) - p(5)]/[t(6) - t(5)] = -\rho(1)c^2(1)\beta_i(6)\beta_j(6)\,\partial u_i/\partial x_j(1) - \rho(2)c^2(2)\alpha_i(6)\alpha_j(6)\,\partial u_i/\partial x_j(2) + \rho(5)c^2(5)[\alpha_i(6)\alpha_j(6) + \beta_i(6)\beta_j(6)]\,\partial u_i/\partial x_j(5) \quad (35)$$

Equations (33–35) and finite-difference forms of Eqs. (12, 13, and 14) form an independent set of six equations.

Like Methods 1 and 2, Method 3 is basically a predictor-corrector scheme. A first-order predictor is used to compute a tentative solution and a second-order corrector is then used to compute the final solution. As in Methods 1 and 2, the solutions are computed on constant x planes located by the C-F-L stability criterion.

Predictor

The streamline is extended from point (5) to the predetermined solution plane using the following finite-difference form of Eq. (10):

$$2[x_i(6) - x_i(5)] = [u_i(6) + u_i(5)][t(6) - t(5)] \quad (i = 1, 2, 3) \quad (36)$$

where $u_i(6)$ is set equal to $u_i(5)$. The four bicharacteristics are then extended back to intersect the initial-value plane. The points of intersection are computed from the following finite-difference form of Eq. (29):

$$2[x_i(6) - x_i(k)] = [u_i(6) + c(6)\alpha_i(6)\cos\theta(k) + c(6)\beta_i(6)\sin\theta(k) + u_i(k) + c(k)\alpha_i(6)\cos\theta(k) + c(k)\beta_i(6)\sin\theta(k)][t(6) - t(k)] \quad (i = 1, 2, 3) \quad (37)$$

where the index k denotes values at the base points (1), (2), (3), and (4), and which correspond to values of $\theta(k)$ equal to 0, $\pi/2$, π, and $3\pi/2$, respectively (see Fig. 2). The values of the properties and derivatives of the properties at points (1)–(4) are determined by interpolation as in Methods 1 and 2. For reasons of numerical stability interpolated property values were also used at point (5). The values of the properties at point (6) in Eq. (37) are set equal to the values at point (k). The α_i and β_i unit vectors are chosen in a plane normal to the velocity vector. Their orientation on this plane is specified such that their projections on the initial-value plane are bisected by the projection of the pressure gradient (see Ransom et al.[23]). It was found during source flow accuracy studies that it is not necessary to correct the location of the base point as was done in Methods 1 and 2.

The values of $u_i(6)$, $p(6)$, $P(6)$, and $H(6)$ are then computed by solving the following finite-difference forms of Eqs. (12, 13, and 14):

$$2[p(6) - p(5)] + [\rho(6)u_i(6) + \rho(5)u_i(5)][u_i(6) - u_i(5)] = 0 \quad (38)$$

$$P(5) = P(6) \quad (39)$$

$$H(5) = H(6) \quad (40)$$

and Eqs. (33–35) where again the value of the properties at point (6) in the coefficients are set equal to the value of the properties at point (5).

The boundary point scheme is the same as the interior point scheme except that Eq. (29) for $\theta = 3\pi/2$ is replaced by the condition that point (6) must lie on a prescribed surface and Eq. (34) is replaced by

$$\bar{n}_i(6)u_i(6) = 0 \quad (41)$$

where $\bar{n}_i$ is the unit outer normal to the boundary at point (6).

Corrector

The corrector uses the same finite-difference equations as the predictor, except now the value of the properties at point (6) in the equation coefficients are those values computed by the predictor. The corrector then follows the same procedure as the predictor and is either applied once or iterated until a convergence criterion is satisfied for each new solution point.

Stability

For all three methods, the C-F-L stability criterion was found to be a necessary condition for stability. The domain of dependence of the difference equations for all three methods was considered to be the convex hull of the eight neighboring mesh points of points (4) and (5) in Figs. 1 and 2, respectively. However, the corrector of Method 1, by using data in the solution plane, enlarges this domain of dependence to include 24 neighboring mesh points in the initial-value surface, while the x step (time-like direction) remains unchanged.

While the C-F-L stability criterion was found to be necessary for stability, Ransom et al.[23] showed that in the case of Method 3 the C-F-L criterion was not sufficient. In fact, Ransom et al.[23] found Method 3 to be only marginally stable (i.e., instabilities appeared after 20 to 30 solution planes were computed) when actual streamline data were used at point (5) in Fig. 2. A linear stability analysis indicated that interpolated streamline data should be used at point (5) instead of the actual data. With this slight modification, the scheme was found to be stable. Therefore, interpolated streamline data were used in all three methods.

Spherical Source Flow Results

To study the accuracy of Methods 1, 2, and 3, spherical source flow in a 15°, axisymmetric, conical nozzle was computed and the solution compared with the exact solution. To save computing time, two planes of symmetry were assumed; therefore, only the positive y, z quadrant was computed. Before comparing the three methods, it was decided to see if the correctors should be applied once or iterated until the solution has converged. In one-dimensional problems (ordinary differential equations) it is usually more efficient to decrease the mesh spacing rather than iterate the corrector. In two-dimensional problems when the mesh spacing is halved, the number of points increases by a factor of 4 instead of 2 as in the one-dimensional case. Therefore, in two-dimensional problems it is not clear which technique is more efficient. For two-dimensional and axisymmetric, steady, isentropic, nozzle flows Hoffman[25] showed that iteration, in general, was not as efficient as correcting once, except in flows with high gradients where two applications of the corrector were sufficient. In three-dimensional problems when the mesh spacing is halved, the number of points increases by a factor of 8 and, therefore, it was felt that these two techniques should be investigated. Figure 3 shows the pressure error vs axial distance for a typical interior streamline using a uniform grid which has 6 mesh points on the positive y or z axis, that is, 36 mesh points in the positive y, z quadrant. The notation (1-PC) denotes Method 1 with the predictor and corrector applied once, where (1-ITER) denotes Method 1 with the predictor applied once and the corrector applied until the solution has converged. A fractional convergence tolerance of 0.0001, which resulted in approximately four applications of the corrector, was used. The computing times in seconds on a CDC 6500 computer are shown at the top of Fig. 3. From Fig. 3, we see that Method 2 has the same level of accuracy as Methods 1 and 3 only when Method 2 was iterated and Methods 1 and 3 were not. The corrector of Method 1 was by far the most time consuming and, therefore, it was found that, in general, the corrector should be applied only once or twice. The corrector of Method 2 required less time than that of Method 1, but slightly more than that of Method 3. Since Method 2, as we shall later see, had first-order accuracy for all

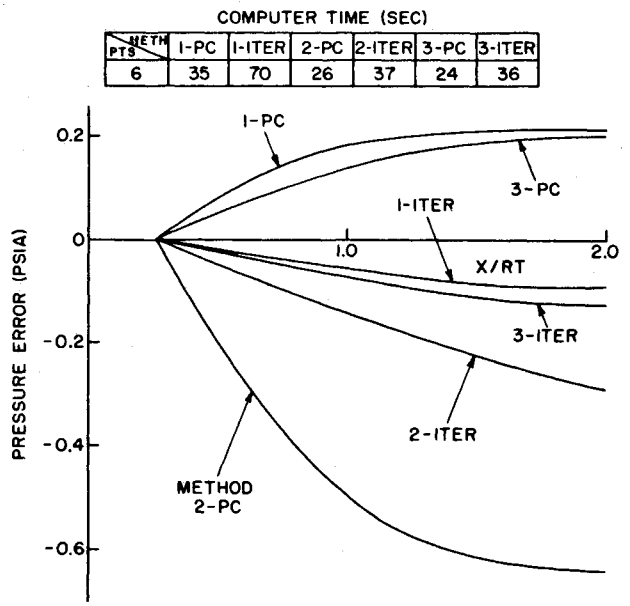

Fig. 3 Effect of corrector iteration on accuracy for spherical source flow.

flows studied, it was found that, in general, it was more efficient to iterate the corrector. The corrector of Method 3 required the least amount of time, yet, in general, it was more efficient to predict and correct once, except for flows with high gradients such as flows where the Mach number approaches unity. For these flows it was more efficient to correct twice, but never more than twice. Therefore, for this study the correctors of Methods 1 and 3 were applied only once and that of Method 2 was iterated approximately four times. In all three methods, iteration of the corrector failed to change the order of accuracy of the method over that obtained by correcting once.

Figure 4 shows the pressure error vs axial distance for a typical interior streamline using uniform grids which have 6, 11, and 21 points on the positive y or z axis. The computing times in seconds are shown at the top of Fig. 4. The notation (1-6) denotes Method 1 using a uniform grid of 6 points on the positive y or z axis. The accuracy of Methods 1 and 3 is approximately the same, although Method 1 requires approximately 50% more computing time. Method 2 for 11 points has approximately the same level of accuracy as Method 3 for 6 points, but requires over seven times the computing time. Since the mesh spacing is approximately halved when the number of points on the positive y or z axis is increased from 6 to 11 or from 11 to 21, the error should be approximately reduced by one-half for first-order schemes and one-fourth for second-order schemes. Therefore, from Fig. 4, Methods 1 and 3 appear to have second-order accuracy whereas Method 2 appears to be first-order. This was found to be the case for all flows considered. In Figs. 3 and 4 the initial Mach number on the centerline was 2.0. Similar results were obtained for an initial Mach number 1.1. The stagnation pressure and enthalpy were 1000 psia and 1255 B/lbm, respectively.

Last of all, an investigation of the efficiency gained (if any) by using a corrector in Methods 1 and 3 to increase the order of accuracy from 1 to 2 was made. Since the corrector of Method 1 required the most computing time, it was decided to compare the accuracy of Method 1 with and without correcting for several mesh spacings. Figure 5 shows the pressure error vs axial distance for a typical interior streamline for both cases. The computing times in seconds are shown at the top of Fig. 5. The three lower curves are Method 1 without correcting for 6, 11, and 21 mesh points on the positive y or z axis and the top curve is Method 1 with correcting for 6 points on the positive y or z axis. From Fig. 5, for Method 1 without correcting to have approximately the same level of accuracy as Method 1 correcting once, Method 1 without correcting would need approximately 41 mesh points on the positive y or z axis and over 100 times the computing time. Therefore, when good accuracy is desired, the correctors of Methods 1 and 3 are well worth the added complexity.

Axisymmetric Flow Results

As a further check on the accuracy of Methods 1, 2, and 3, these methods were used to compute the axisymmetric, steady, isentropic flow of a thermally and calorically perfect gas in a parabolic nozzle. These solutions were compared with that of an axisymmetric method of characteristics program. The nozzle selected was a circle-parabola contour with a 1-in. throat radius, 1-in. throat radius of curvature, 30° tangency angle, 15° exit angle, and a length of 10 in. The initial-value plane was assumed

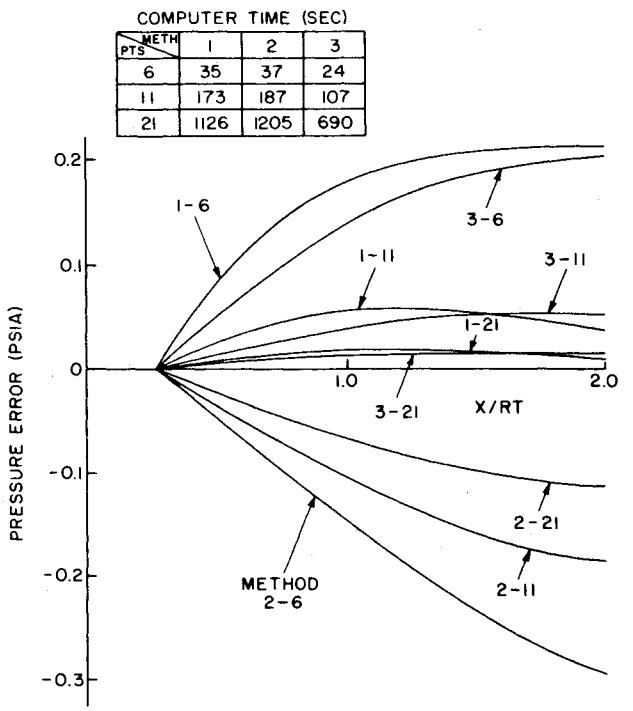

Fig. 4 Effect of mesh spacing on accuracy for spherical source flow.

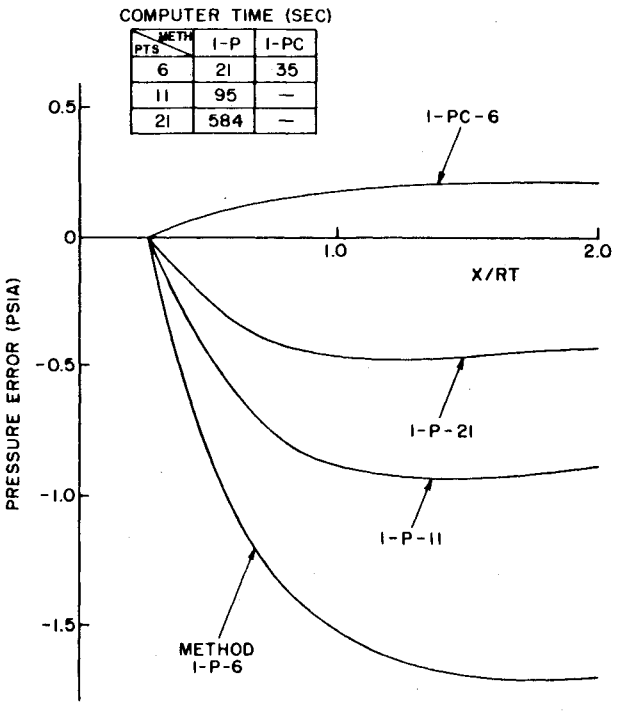

Fig. 5 Effect of the corrector on accuracy for spherical source flow.

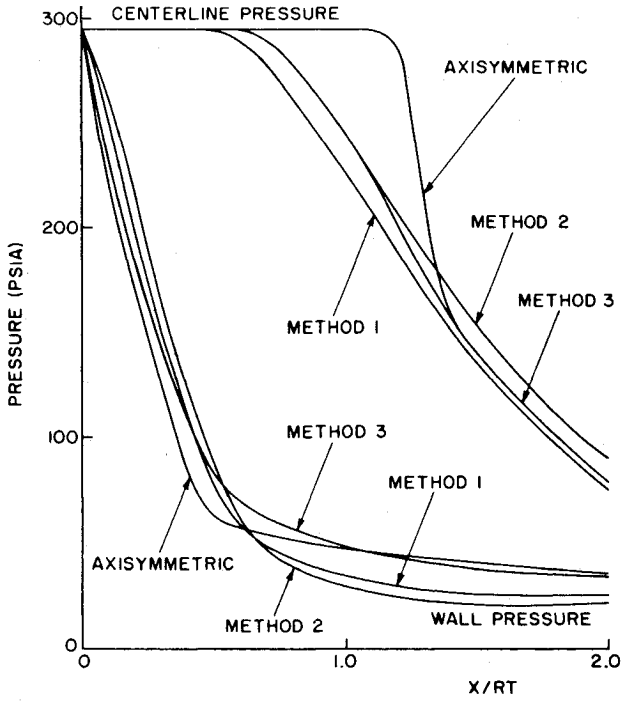

Fig. 6 Comparison of the two- and three-dimensional methods for flow in an axisymmetric parabolic nozzle.

to be uniform flow at a Mach number of 1.5. The axisymmetric method used 41 points on the initial-value line (positive y axis), while the three-dimensional methods used 6 and 11 points on the positive y or z axis. Again, two planes of symmetry were assumed and, therefore, only the positive y, z quadrant was computed by the three-dimensional methods.

Figure 6 shows the pressure versus axial distance for both wall and centerline streamlines for a mesh spacing of 6 points on the positive y or z axis. From Fig. 6, it is seen that on the center line Method 3 produced a solution that was closest to the axisymmetric solution. The large differences between the three-dimensional methods and the axisymmetric method is due to the rather coarse grid used by the three-dimensional methods. The three-dimensional methods using 11 points on the positive y or z axis gave results (not shown) much closer to the axisymmetric solution. Method 3 was again the closest to the axisymmetric method on the wall. The differences between the three-dimensional methods using six points on the positive y or z axis and the axisymmetric method along with the computing times for the wall streamline are shown in Fig. 7.

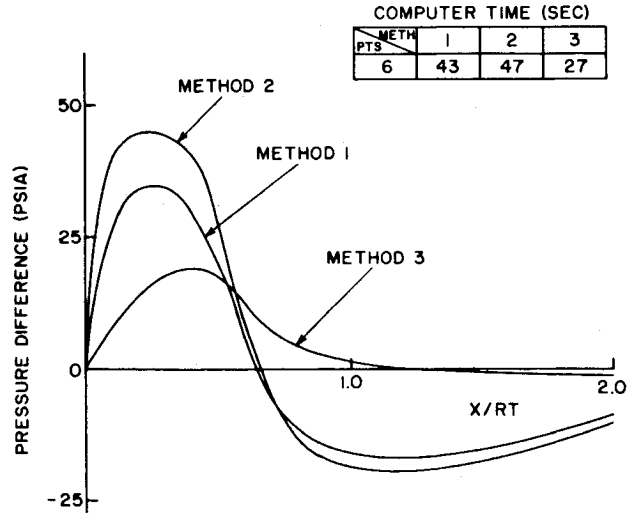

Fig. 7 Wall-pressure difference between the two- and three-dimensional methods for flow in an axisymmetric parabolic nozzle.

Conclusions

All three methods were found to be numerically stable and able to produce efficient and accurate solutions. Since all three methods had merit, the selection of one scheme over the others may well depend on the problem to be solved as well as the computer on which the calculations will be carried out. For the case of three-dimensional, steady flow, some general conclusions have been drawn and are presented.

Methods 1 and 2 are conceptually the simplest as well as being slightly easier to program. All three methods used data slightly outside the domain of dependence of the differential equations when interpolating for the properties and cross derivatives at the base points formed by the intersection of the bicharacteristics and the initial-value plane. In addition, the corrector of Method 1 used data in the solution plane to interpolate for the cross derivatives at the solution point. Therefore, Methods 2 and 3 more rigorously treat the domain of dependence. On the other hand, Methods 1 and 3 more rigorously treat the cross derivatives and, therefore, have second-order accuracy, whereas Method 2 appears to be a first-order scheme. From the results of the source and axisymmetric flow accuracy studies discussed above, Method 3 appears to be, in general, the most accurate and efficient scheme.

Therefore, when conceptual simplicity and ease of programing are the main objectives, Method 1 or 2 may be a good choice. But, in general, it is felt that the better accuracy and efficiency of Method 3 outweigh its complexity. Therefore, Method 3 is recommended as the best over-all scheme.

References

[1] Ferrari, C., "Interference Between Wing and Body at Supersonic Speeds—Analysis by the Method of Characteristics," *Journal of the Aeronautical Sciences*, Vol. 16, July 1949, pp. 411–434.

[2] Sauer, R., "Application of Characteristic Theory for Partial Differential Equations to the Solution of Problems Arising in Three-Dimensional Flow," *Zeitschrift für Angerwandte Mathematik und Mechanik*, Vol. 30, Nov. 1950, pp. 347–356.

[3] Sauer, R., "The Method of Finite Differences for the Initial-Value Problem," *Numerische Mathematik*, Vol. 5, 1963, pp. 55–67; translated by K. N. Trirogoff, Literature Research Group, Aerospace Library Services, Aerospace Corp., San Bernardino, Calif.

[4] Ferri, A., "The Method of Characteristics," *General Theory of High Speed Aerodynamics*, Vol. VI, edited by W. R. Sears, 1954, Princeton University Press, Princeton, N. J., pp. 583–669.

[5] Moretti, Gino, "Three-Dimensional Supersonic Flow Computations," *AIAA Journal*, Vol. 1, No. 9, Sept. 1963, pp. 2192–2193.

[6] Moretti, G. et al., "Supersonic Flow About General Three-Dimensional Blunt Bodies," ASD-TR-61-727 Vol. I, II, and III, Contract AF 33 (616)-7721, Oct. 1962, General Applied Science Lab., Westbury, N. Y.

[7] Katskova, O. N. and Chushkin, P. I., "Three-Dimensional Supersonic Equilibrium Flow of a Gas Around Bodies at Angles of Attack," TT F-9790, 1965, NASA.

[8] Holt, M., "Recent Contributions to the Method of Characteristics for Three-Dimensional Problems in Gas Dynamics," Feb. 26, 1963, Space General Corp., El Monte, Calif.

[9] Holt, M., "The Method of Near Characteristics for Unsteady Flow Problems in Two Space Variables," Rept. AS-63-2, June 1963, Contract Nonr-222 (79), Inst. of Engineering Research, Univ. of California.

[10] Rakich, J. V., "A Method of Characteristics for Steady Three-Dimensional Supersonic Flow With Application to Inclined Bodies of Revolution," TN D-5341, 1969, NASA.

[11] Chushkin, P. I., "Numerical Method of Characteristics for Three-Dimensional Supersonic Flows," *Progress in Aeronautical Science*, Vol. 9, edited by D. Kuchemann, Pergamon Press, New York, 1968, Chap. 2.

[12] Thornhill, C. K., "The Numerical Method of Characteristics for Hyperbolic Problems in Three Independent Variables," ARC Rept. and Memo. 2615, Sept. 1948, London, England.

[13] Fowell, L. R., "Flow Field Analysis for Lifting Reentry Configurations by the Method of Characteristics," *IAS Paper 61-208-1902*, June 13–16, 1961.

[14] Sauerwein, H., "The Calculation of Two- and Three-Dimensional Inviscid Unsteady Flows by the Method of Characteristics," Ph.D. thesis, June 1964, MIT, Cambridge, Mass.

[15] Sauerwein, H., "Numerical Calculations of Arbitrary Multidimensional and Unsteady Flows by the Method of Characteristics," AIAA Paper 66-412, Los Angeles, Calif., 1966.

[16] Coburn, N. and Dolph, C. L., "The Method of Characteristics in the Three-Dimensional Stationary Supersonic Flow of a Compressible Gas," *Proceedings of the First Symposia on Applied Mathematics, American Mathematical Society*, New York, 1949.

[17] Holt, M., "The Method of Characteristics for Steady Supersonic Rotational Flow in Three Dimensions," *Journal of Fluid Mechanics*, Vol. 1, 1956, p. 409.

[18] Butler, D. S., "The Numerical Solution of Hyperbolic Systems of Partial Differential Equations in Three Independent Variables," *Proceedings of the Royal Society of London*, 255A, 1960, p. 232.

[19] Strom, C. R., "The Method of Characteristics for Three-Dimensional Steady and Unsteady Reacting Gas Flows," Ph.D. thesis, Jan. 1965, Univ. of Illinois.

[20] Chu, C.-W., "Compatibility Relations and a Generalized Finite Difference Approximation for Three-Dimensional Steady Supersonic Flows," *AIAA Journal*, Vol. 5, No. 3, March 1967, pp. 493–501.

[21] Cline, M. C. and Hoffman, J. D., "The Analysis of Nonequilibrium, Chemically Reacting, Supersonic Flow in Three Dimensions, Vol. I, Theoretical Development and Results," Rept. AFAPL-TR-71-73, Air Force Aero Propulsion, Wright-Patterson Air Force Base, Ohio, Aug. 1971, Appendix IV.

[22] Rusanov, V. V., "The Characteristics of General Equations of Gas Dynamics," *Zhurnal Vyschislitel'noi Matematiki Matematicheskoi Fiziki*, Vol. 3, No. 3, 1963, pp. 508–527; translated by Trirogoff, K. N., LRG-65-T-38, Literature Research Group, Aerospace Corp., San Bernardino, Calif.

[23] Ransom, V. H., Hoffman, J. D., and Thompson, H. D., "A Second-Order Numerical Method of Characteristics for Three-Dimensional Supersonic Flow, Vol. I, Theoretical Development and Results," Rept. AFAPL-TR-69-98, Oct. 1969, Air Force Aero Propulsion Lab., Wright-Patterson Air Force Base, Ohio.

[24] Butler, D. S., private communication, Oct. 1968.

[25] Hoffman, J. D., "Accuracy Studies of the Numerical Method of Characteristics for Axisymmetric, Steady Supersonic Flows," *Journal of Computational Physics*, to be published.

NOVEMBER 1972 AIAA JOURNAL VOL. 10, NO. 11

Lee-Side Vortices on Delta Wings at Hypersonic Speeds

DHANVADA M. RAO* AND A. H. WHITEHEAD JR.†
NASA Langley Research Center, Hampton, Va.

A fluid-dynamic investigation was carried out to determine the cause of intense heating observed on the lee meridian of hypersonic delta wings and also to derive means for its suppression. Several experimental techniques were combined with analysis of extensive heat-transfer measurements at $M_\infty = 6$ in a range of Reynolds number to acquire a general description of the lee-flow structure. With attached leading-edge flow on the delta wings, the dominant feature is a pair of embedded vortices on the lee meridian whose interaction with the boundary-layer is responsible for the observed local heating. On the basis of flow visualization results and heat-transfer correlations, a qualitative vortex flow model is proposed which differs essentially from the conventional inboard separation vortex model. This approach leads to successful methods for alleviation of vortex heating. The proposed concept of boundary-layer embedded vortices also appears to explain the hypersonic lee-side heating characteristics observed on a shuttle oribiter configuration.

Nomenclature

M_∞ = freestream Mach number
P_∞ = freestream impact pressure
P' = local impact pressure
R_∞ = freestream unit Reynolds number
$R_x = x \cdot R_\infty$
$R_{x'} = (x - x^*)R_\infty$
R_L = model length Reynolds number
St_∞ = Stanton number based on freestream conditions
x = coordinate along center line from apex (or nose), positive downstream
x^* = distance along x to peak heating (or other flow characteristic)
x' = coordinate along center line, originating at $x = x^*$
y = spanwise coordinate from center line
z = coordinate normal to planar upper wing surface, positive upward
α = incidence angle of upper planar surface, positive leeward
α_0 = incidence relative to model reference axis
Δ = width of vortex trace in oil pattern (Fig. 3)
δ = boundary-layer thickness in plane of symmetry
θ = angle between vortex trail and wing center line (Fig. 3)
Λ = leading-edge sweep-back angle
ϕ = mayimum outflow angle in vortex trace (Fig. 3)

Received March 27, 1972; revision received June 16, 1972. Part of this work was done under a NRC/NASA Post-Doctoral Research Associateship with Configuration Flow Fields Section, Hypersonic Vehicles Division.

Index categories: Airplane and Component Aerodynamics; Supersonic and Hypersonic Flow; Jets, Wakes, and Viscid-Inviscid Flow Interactions.

* Research Associate; presently at Aerodynamics Division, National Aeronautical Laboratory, Bangalore, India. Member AIAA.

† Aerospace Engineer, Configuration Flow Fields Section, Hypersonic Vehicles Division. Associate Member AIAA.

Introduction

IN the extensive research on hypersonic aerodynamics of delta wings, the leeward flowfield has so far received limited attention. Although lee surface pressures contribute the smallest part to the aerodynamic loads at high Mach numbers, vortex phenomena have been found responsible for intense local heating over the lee meridian of delta wings (peaking to more than three times the two-dimensional laminar estimates),[1] and also on hypersonic configurations such as the space shuttle.[2] Since such heating could constitute a potential design problem for hypersonic vehicles in sustained cruising flight, the need for improved prediction of the lee-side heating is indicated. For this purpose and also to explore aerodynamic means for its suppression, a basic study of the leeward vortex phenomena seems necessary.

Limited lee-side data have prompted the previous investigators[3-10] of supersonic delta wing flow to discuss their results in terms of vortex flow models derived from studies at lower Mach numbers. The well-known vortex flow resulting from leading-edge separation (Fig. 1A) has been found valid at supersonic freestream Mach numbers so long as the velocity component normal to the leading edge remains well below the sonic value.